ENVIRONMENTAL IMPACTS AND BENEFITS OF STORMWATER RUNOFF TREATMENT ACROSS THE LIFE CYCLE OF BIORETENTION TANKS

WU, S. X.[1] – JIANG, C. B.[2*] – LI, H. E.[2] – DANG, Z. G.[1]

[1]*Department of Municipal and Environmental Engineering, Xi'an University of Technology, Xi'an, Shaanxi 710048, China*
(e-mail: 1243789819@qq.com (Wu, S. X.), 975541282@qq.com (Dang, Z. G.))

[2]*State Key Laboratory of Water Engineering Ecology and Environment in Arid Area, Xi'an University of Technology, Xi'an 710048, China*
(e-mail: lhuaien@mail.xaut.edu.cn)

[*]*Corresponding author*
e-mail: chunbo@xaut.edu.cn

(Received 2nd May 2025; accepted 26th Jun 2025)

Abstract. Bioretention is extensively used for efficient and cost-effective stormwater treatment. Current research primarily focuses on isolated factors such as water purification efficiency and infiltration rate variations in bioretention cells. A life cycle assessment system has been established to evaluate the positive and negative environmental impacts of the system, from resource acquisition, transportation, and construction to operation, demolition, and disposal. By conducting environmental benefit monetization calculations, the evaluation indicator system for the construction effectiveness of bioretention cell systems has been improved. Following 20 years of local rainfall simulation and 40 simulated rainfall events in three stages, accompanied by tests for soil hydraulic conductivity curves, particle distribution, and pollutant contents, the variation pattern of effluent concentration was described, and an exponential relationship between operational time and stable infiltration rate ($R^2 > 0.905$) was established. A life cycle assessment framework was established using experimental data and OpenLCA software, with characterization indicators covering acidification, carcinogenic emissions, eutrophication, fossil fuel consumption, greenhouse effect, non-carcinogenic emissions, ozone depletion, and respiratory impacts. Based on the variation in the stable infiltration rate, the study determined that the lifespan of bioretention cell systems ranges from 16.2 to 26.8 years. The environmental negative impacts are highest during the raw material acquisition and construction phases, accounting for 77% to 79%. The environmental positive impacts are highest during the modified media recycling and reuse phase, accounting for 61% to 80%. The monetized benefits range from 49.61 to 77.44 $EUR \cdot m^{-3}$ over the entire life cycle of bioretention cell systems.
Keywords: *stormwater, improved media, life cycle assessment, hydraulic conductivity, environmental impact*

Introduction

The frequency of extreme weather events and the severity of flood disasters have increased due to the combined effects of global climate change and rapid urbanization. This escalation poses significant challenges to sustainable development and economic growth worldwide. Bioretention cells are plant-filters designed to capture, percolate, and purify stormwater runoff by leveraging a series of physical, chemical, and biological processes. Existing research focuses on purification mechanisms, infiltration improvement, model simulations, and benefit evaluations (Lisenbee et al., 2021; Vijayaraghavan et al., 2021; Chen et al., 2022). The composition of bioretention soil media (BSM) varies depending on the national, industrial, and regional design objectives and regulations, as well as the cost and availability of local BSM sources, Design considerations for bioretention cells include filler type and depth, plant species, internal

http://www.aloki.hu ● ISSN 1589 1623 (Print) ● ISSN1785 0037 (Online)
DOI: http://dx.doi.org/10.15666/aeer/2304_83178334

storage zones, and structural settings. Among these, the filler plays the most important role (Tirpak et al., 2021). BSM typically consists of sandy soil blended with an organic amendment such as compost, wood chips, bark fines, or topsoil (Li and Davis, 2008a,b; Wardynski and Hunt, 2012; Wan et al., 2017). An improved filler demonstrates effective control over water quantity and quality. However, the system's operation may give rise to various issues over time (Iqbal et al., 2015; Nabiul et al., 2017; Guo et al., 2018). Clogging can decrease the system's hydraulic conductivity, leading to increased drawdown times, a higher frequency of overflow, and the formation of highly polluted layers (Hatt et al., 2007; Ding et al., 2019). Factors influencing media clogging include inflow hydraulics and pollution load, mixed filler structure and characteristics, and plant species. Research on the temporal-spatial variation of hydraulic conductivity in media and its relationship with particle size distribution and porosity is limited. Further research is needed on predictive models and control measures for the clogging process of modified bioretention media.

During the continuous operation of bioretention cells, the filtration media accumulate pollutants gradually from runoff, leading to a reduction in hydraulic conductivity and causing clogging, until the system is decommissioning and recycling. Current research has explored the potential of bioretention cells in stormwater treatment but has not considered the environmental impacts related to the resource acquisition, transportation, construction, operation, demolition and disposal of the system (Brudler et al., 2016). Currently, Various studies involve full lifecycle environmental impact assessment (Pourmehdi and Kheiralipour, 2023; Kheiralipour et al., 2023; Coelho et al., 2024; Xu et al., 2024). Consider the application of relevant methods in the runoff regulation process for low impact development facilities, Flynn and Traver (2013) evaluated the environmental impacts of bioretention facilities and green roofs during their construction, and decommissioning phases under the premise that the life cycle is thirty years, focusing on global warming potential, carcinogens, eutrophication, and ecotoxicity. They also predicted the annual carbon storage and sequestration potential of the vegetation in bioretention facilities. Moore and Hunt (2013) conducted a life cycle assessment of various types of low impact development (LID) facilities under the premise that the life cycle is forty years, quantifying the carbon emissions during both the construction and operation phases of these infrastructures. Existing studies on the benefits of stormwater management measures often select a limited range of indicators. The majority are greenhouse gas emissions, and carbon emissions equivalent is used as the evaluation factor. A standardized approach to define the lifespan of stormwater ecological treatment facilities is lacking and insufficient. For bioretention systems, the environmental impacts resulting from differences in pollutant retention efficiency and lifespan of solid waste application have not yet been considered.

This research aims to investigate the clogging process of typical modified bioretention cells. The analysis leverages a laboratory-based, column-scale study replicating 20 years of runoff volume, and environmental impact assessment based on OpenLCA software. The study seeks to address the following objectives: i) determine the expected rate of hydraulic conductivity due to temporal-spatial changes, ii) identify the trends of the main factors (such as particle size distribution and pollutant content) that impact the decline of hydraulic conductivity, and iii) Conduct an environmental impact assessment of bioretention cells with modified media from a full life cycle perspective. This research provided guidance and a theoretical foundation for ensuring the sustainability and environmental effects of improved bioretention cells.

http://www.aloki.hu ● ISSN 1589 1623 (Print) ● ISSN1785 0037 (Online)
DOI: http://dx.doi.org/10.15666/aeer/2304_83178334

Materials and methods

Experimentation materials and methods

Experimental set up

To understand the degradation process of infiltration performance for solid waste modified bioretention media, six columnar structures (10 cm diameter and a depth of up to 65 cm) were constructed as shown in *Figure 1*. Each column was composed of several distinct layers, starting from the top with an ultra-high layer (3 cm), followed by an ponding depth (5 cm), a mulch layer (2 cm), the mixed media (50 cm), and finally a gravel drainage layer (5 cm). A layer of bark (2 cm) on the surface of the media was added to enhance preferential flow, facilitating hydraulic energy dissipation and uniform water distribution. Each media component was mixed evenly, filled densely, and compacted to minimize pore formation.

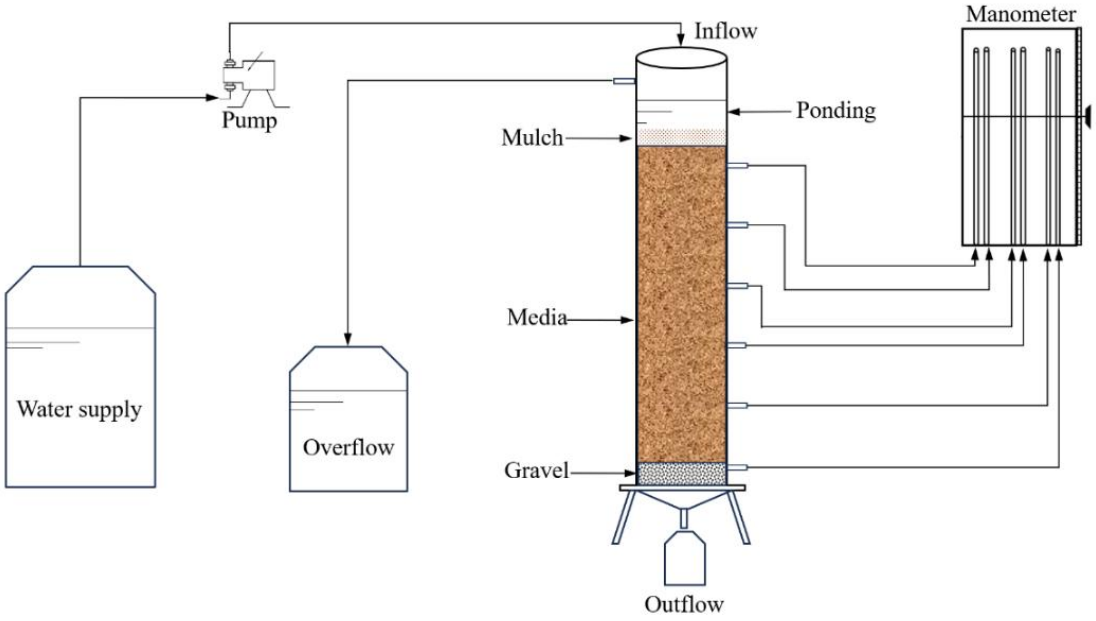

Figure 1. *Bioretention simulation tank*

The media layer was prepared by mixing a basic filler (river sand, planting soil and compost) with fly ash, biochar, water treatment residues (WTR), and recycled aggregate of construction waste (RACW) in varying proportions (*Table 1 & Table 2*). The solid waste modifier was generated through air-drying, granulation, pyrolysis, and decay. The average unit weight of the filler layer was 1.3 g/cm^3, with a total mass of 5102.5 g. Six pressure measuring holes were distributed from top to bottom at 10 cm intervals on the side of the device.

This study conducted a simulation of surface runoff based on relevant design guidelines and actual rainfall magnitude observed in Xi'an, Shaanxi province, China. This experiment divides the water inflow process into three stages, which is based on the sum of rainfall in dry, normal, and wet years in the 20-year rainfall data of the study area as a reference, respectively. And the annual rainfall and rainfall duration are respectively 446.5, 536.2, and 636.5 mm, 6, 9, and 5 years.

http://www.aloki.hu ● ISSN 1589 1623 (Print) ● ISSN1785 0037 (Online)
DOI: http://dx.doi.org/10.15666/aeer/2304_83178334

Table 1. *Improved media ratio and composition (by mass)*

No.	Media	Modifier parameters
1	BSM	(river sand: planting soil=7:3): yard compost=97:3 mass ratio
2	BSM+10% flyash	Waste from coal-fired power plants Particle size: 8~12μm
3	BSM+3% biochar	Straw-based biochar ,0~2mm
4	BSM+10%RACW	mortar, ceramic fragments, and concrete blocks Particle size: 1~2mm
5	BSM+5%WTR-1	Natural air-drying, 1~2mm
6	BSM+5%WTR-2	WTR-based biochar, 1~2mm

Note: WTR-1&WTR-2 are water treatment residuals which is natural air-dried granulation and air-dried; and RACW is recycled aggregate of construction waste

Table 2. *Basic characteristics of modifiers*

Modifier	LC	Biochar	WTR-1	WTR-2	Flyash	RACW
pH	7.95	9.00	7.94	7.80	9.50	9.20
EC (us/cm)	994.89	6335.93	376.79	410.03	1235.16	494.06
BET (m^2/g)	4.73	14.70	25.97	256.10	1.95	2.53
CEC (cmol/kg)	40.00	10.70	42.80	24.90	3.00	7.20

Note: EC is conductance; BET is specific surface area; CEC is cation exchange capacity; LC is Leaf compost; Biochar is corn stalk biochar; WTR-1&WTR-2 are water treatment residuals which is natural air-dried granulation and air-dried; And RACW is recycled aggregate of construction waste

The distribution of total rainfall volume in the three stages was calculated by multiplying the rainfall intensity by the comprehensive runoff coefficient and the catchment area (*Equation 1*). The total amount of water inflow in each stage is 315.4 L, 568.3 L, and 374.8 L. For the calculation of inflow velocity, design rainfall recurrence interval were set at 1a, 2a, and 3a with a consistent duration of 60 minutes for each rainfall event. Rainfall intensity for individual events was determined based on the storm intensity equation.

$$V = 10^{-3} DF\varphi \quad \text{(Eq.1)}$$

where, V is the design runoff volume,m^3; φ is the comprehensive runoff coefficient; D is the rainfall (mm); F is the catchment area of the facility, m^2.

As a result, the rainfall intensity gradually increased through the three stages, reaching 34.74 mL/min, 46.86 mL/min, and 54.05 mL/min, respectively. Each device received inflow for 12 hours, followed by a 12-hour shutdown to prevent overflow. A total of 40 simulated rainfall events were conducted, divided into 13, 17, and 10 events per stage. A 4-day interval was observed after completing the rainfall events in each stage (*Table 3*). According to the concentration characteristics of road runoff in Xi'an, the synthetic stormwater concentration is prepared as follows: SS (300 mg/L), COD (300 mg/L), NO_3-N (3 mg/L), NH_3-N (4 mg/L), TP (1.2 mg/L), Cu (0.5 mg/L), Zn (1.5 mg/L), Cd (0.3 mg/L). The preparation method for TSS is as follows: Collect sediment from the inflow weir of an on site bioretention facilities, then after naturally drying the sediment, pass it through a standard 60-mesh screen, and finally prepare a solution with a

http://www.aloki.hu ● ISSN 1589 1623 (Print) ● ISSN1785 0037 (Online)
DOI: http://dx.doi.org/10.15666/aeer/2304_83178334

concentration of 300 mg/L. The reagents used for remaining preparations were glucose, KNO_3, NH_4Cl, KH_2PO_4, $CuCl_2$, $ZnSO_4$ and $CdCl_2$.

Table 3. *Inflow design*

Levels	Rainfall (mm)	Design period (year)	Facility area (cm^2)	Confluence ratio	Volume (L)	Total volume (L)
Dry year	446.49	6	78.5	15:1	315.4	1258.5
Normal year	536.23	9			568.3	
Wet year	636.53	5			374.8	

Note: The catchment area ratio (catchment area/facility area) of bioretention facilities is 5:1-20:1, and this study selected 15:1

Detection indexes and methods

The parameters of this study include influent and effluent water quality indices, filler composition and particle grading, and the temporal-spatial variation process of infiltration capacity. Water samples, each comprising 500 mL, were collected twice a day on average and stored at 4°C, with detection completed within a 24-hour timeframe. The media sample was obtained through destructive sampling; to minimize interference with the hydraulic conductivity characteristics of the filler material, sampling was conducted only before and after the entire set of tests. Media samples were collected in layer segments (0~10 cm, 10~20 cm, 20~30 cm, 30~40 cm, 40~50 cm), air-dried in a well-ventilated area, and sealed in polyethylene bottles. The detection indicators included pollutant content (TN, TP, TOC, Cu, Zn, Cd) and particle size distribution. Temporal and spatial changes in hydraulic conductivity were assessed through vertical soil column infiltration experiments and the piezometric tube head method. At the start of the experiment and at each stage of operation, the overall infiltration rate was gauged using the Mariotte flask constant head method (Wang, 2023; Zhang et al., 2025). Simultaneously, the filler was divided into two layers (0~20 cm, 20~50 cm), and the infiltration coefficient of each layer was determined by measuring the piezometer's head and applying Darcy's law. The determination method is shown in *Table 4 and Table 5*.

Table 4. *Test indicators and methods*

Category	Index	Measurement method
Water quality index detection	TN	Alkaline potassium persulfate digestion spectrophotometry
	TP	Potassium persulfate digestion ammonium molybdate spectrophotometry
	COD	Potassium dichromate rapid digestion spectrophotometry
	Cu, Zn, Cd	Flame atomic absorption method
Media sample test	TN	Kjeldahl method
	TP	Molybdenum-antimony anti-spectrophotometry
	TOC	Potassium dichromate oxidation - external heating method
	Cu, Zn, Cd	Modern analytical method of soil elements
	Grain gradation	Marvin 2000 laser particle size analyzer, and triangle map of soil texture in the United States
Infiltration capacity	Temporal process	Martensite flask+infiltration column, constant head method
	Spatial process	Piezometer head, Darcy's law

http://www.aloki.hu ● ISSN 1589 1623 (Print) ● ISSN1785 0037 (Online)
DOI: http://dx.doi.org/10.15666/aeer/2304_83178334

Table 5. *Main instruments and equipment*

Instrument Name	Model	Manufacturer
UV-Vis Spectrophotometer	*DR6000*	*HACH*
Autoclave (Pressure Steam Sterilizer)	*LS-50HD*	*Xinling Instruments*
Peristaltic Pump	*BT100-1L*	*Lange*
Metering Pump	*V-09003*	*Aldos*
Flame Atomic Absorption Spectrometer	*ZEEnit700P*	*Analytik Jena (Germany)*
COD Digester	*DRB200*	*HACH*
Muffle Furnace	*X2-8-13T*	*Jinwen*
Conductivity Meter	*HQ30d*	*HACH*

Environmental impact

The analysis of the list at each stage

The environmental impacts throughout the entire cycle from raw material acquisition, transportation, construction, operation, to demolition and disposal was evaluated, using a "cradle to grave" life cycle assessment method (*Figure 2*).

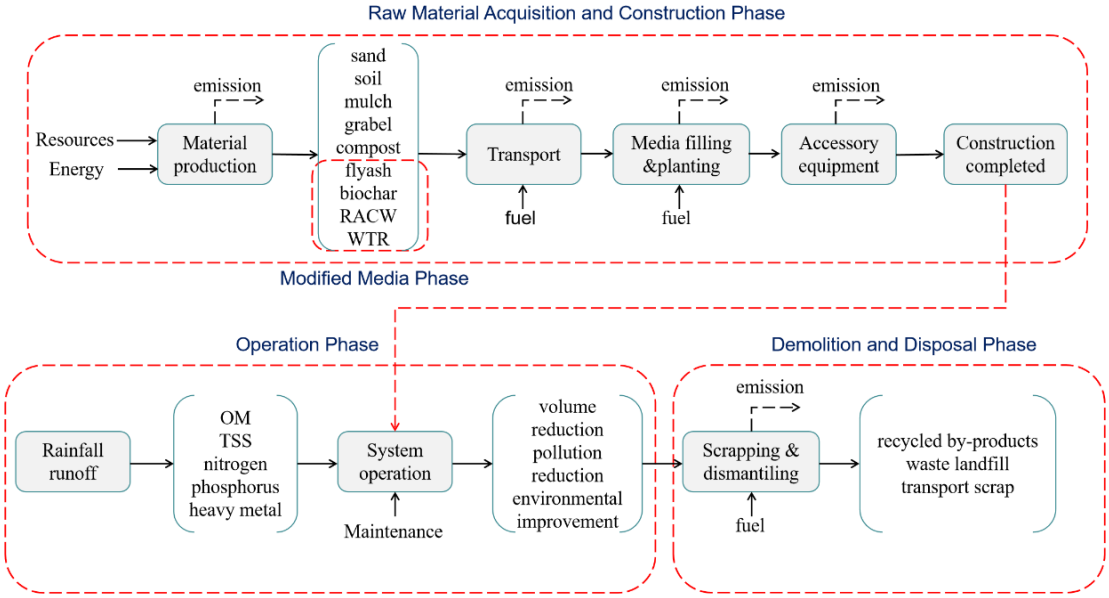

Figure 2. *Life cycle environmental impacts assessment framework*

Raw material acquisition and Construction phase: i) The production and acquisition of bioretention cells fillers generate environmental impacts (excluding the modified media). ii) The environmental impacts generated by material transportation depend on factors such as the choice of transportation vehicles, fuel types, road conditions, and transportation distances. iii) There are also environmental impacts associated with on-site operations, including earthwork excavation, geotechnical support, and the mixing and filling of media materials.

Modified media recycling and reuse phase: in conventional life cycle assessment systems, the acquisition of raw materials typically generates environmental impacts. However, the utilization of recycled solid waste materials -such as industrial byproducts,

http://www.aloki.hu ● ISSN 1589 1623 (Print) ● ISSN1785 0037 (Online)
DOI: http://dx.doi.org/10.15666/aeer/2304_83178334

agricultural residues, and construction debris-as amendments in bioretention systems demonstrates notable environmental benefit. By repurposing materials from waste streams, this approach effectively reduces environmental contamination pressures.

Operation phase: i) The bioretention system regulates runoff rainwater, effectively intercepting organic pollutants, nutrients, heavy metals, etc. in the runoff, reducing environmental pollution emissions, and playing a positive role in plant growth and the healthy cycle of the microecology system. ii) The interception and infiltration of runoff rainwater by bioretention systems help maintain the stability of the groundwater level and enhance the safety of the water environment. iii) During rainfall events, the bioretention systems can reduce runoff volume and peak flow, effectively alleviating the discharge pressure on municipal drainage networks (Li et al., 2021).

Demolition and disposal phase: During the demolition and disposal process, partial materials can be recycled and reused, while others are treated as waste. Typically, the energy consumption involved in this process is estimated based on the corresponding proportions during the construction phase (Liang, 2012).

TRACI 2.1 assessment method

Research employed the TRACI 2.1 (Tool for the Reduction and Assessment of Chemical and other environmental Impacts) methodology within the OpenLCA platform to conduct a life cycle assessment of bioretention cell systems (BSM, BSM + 10% RACW, BSM + 10% flyash, BSM + 3% biochar) (Dhivya et al., 2022). Quantifies the potential environmental impacts of four bioretention systems across eight environmental impact categories from resource extraction, transportation, construction, operation, to demolition and disposal, including acidification, carcinogenic emissions, eutrophication, fossil fuel consumption, greenhouse gas emissions, non-carcinogenic emissions, ozone depletion, and respiratory effects.

Environmental benefit monetization calculations

The environmental benefits generated by the bioretention systems include runoff reduction, reduction of pollution loads, groundwater recharge, rainwater resource recycling, and carbon emission reduction. This paper considers the monetized benefits of bioretention systems from ecological, environmental, and economic perspectives: ① The ecological benefits of bioretention systems include the system's interception and infiltration of stormwater, combined with measures to reduce groundwater extraction, maintaining the stability of the annual average groundwater level, keeping the average decline below the same period in history (Haghani et al., 2013), achieving the goal of preventing groundwater level decline and improving the urban water environment (Moon, 2004). The benefits are calculated through *Equation (2)*; ② The environmental benefits of bioretention systems include the system's filtration and decomposition of pollutants, effectively reducing the pollution levels of urban stormwater runoff. The benefits of water quality purification are assessed by measuring the cost of treating an equivalent amount of pollutants, based on the Second-Class Sewage Discharge Equivalents as stipulated in the Regulations on *the Environmental Protection Tax Law of the People's Republic of China* (Wang, 2008). The benefits are calculated through Equation (3); ③ The economic benefits of bioretention systems include the alleviation of pressure on drainage networks and wastewater treatment plants, as well as the revenue generated from stormwater reuse which are calculated through *Equations (4-6)*. The interpretation of the indicators used in the formula is provided in *Table 6*.

http://www.aloki.hu ● ISSN 1589 1623 (Print) ● ISSN1785 0037 (Online)
DOI: http://dx.doi.org/10.15666/aeer/2304_83178334

$$B_{GWR} = Q_{In} \times P_w = \theta \times \mathrm{D} \times \mathrm{R_v} \times \mathrm{A} \times \mathrm{a_{In}} \times P_w \quad \text{(Eq.2)}$$

$$B_c = P_p \times \sum_i (N_i \times Q_i) = P_p \times \sum_i (N_i \times \theta \times \mathrm{D} \times \mathrm{R_v} \times \mathrm{A} \times \mathrm{a_i} \times C_i) \quad \text{(Eq.3)}$$

$$B_{WDS} = \Delta Q_{Dec} \times P_{WDS} = \theta \times \mathrm{D} \times \mathrm{R_v} \times \mathrm{A} \times \mathrm{a_{Dec}} \times P_{WDS} \quad \text{(Eq.4)}$$

$$B_{WWTP} = \Delta Q_{WWTP} \times \mathrm{P_{WWTP}} = \theta \times \mathrm{D} \times \mathrm{R_v} \times \mathrm{A} \times \mathrm{a_{WWTP}} \times \mathrm{P_{WWTP}} \quad \text{(Eq.5)}$$

$$\mathrm{B_{Rec}} = \mathrm{Q_{Rec}} \times \mathrm{P_W} = \theta \times \mathrm{D} \times \mathrm{R_v} \times \mathrm{A} \times \mathrm{a_{Rec}} \times \mathrm{P_W} \quad \text{(Eq.6)}$$

Table 6. *Definitions and interpretations of the key indicators*

Indicator	Interpretation	Unit
B_{GWR}	the value of maintaining groundwater levels	EUR
Q_{In}	the recharge volume of bioretention system to groundwater	m^3
P_w	the municipal water price	EUR/m^3
θ	the comprehensive runoff coefficient	-
R_v	the annual average runoff reduction rate	-
D	the annual precipitation	mm
A	the catchment area	m^2
a_{In}	the infiltration coefficient	-
B_c	the value of pollutant purification in stormwater runoff by the bioretention system	EUR
P_p	the pollution equivalent charge standard	EUR/equivalent
i	i represents three types of pollutants: SS, COD, and NH_3-N	-
N_i	the pollution equivalent value	-
Q_i	the amount of pollutants treated by the bioretention system	m^3
a_i	the removal rate of each pollutant	-
C_i	the concentration of each pollutant in the stormwater runoff	mg/ml
B_{WDS}	the reduction in sewer maintenance costs	EUR
ΔQ_{Dec}	the change in the sewer flow before and after the operation of bioretention	m^3
P_{WDS}	the cost of sewer maintenance	EUR/m^3
a_{Dec}	the bioretention retention coefficient	-
B_{WWTP}	the change in the cost of stormwater treatment at the wastewater treatment plant before and after the operation of bioretention	EUR
ΔQ_{WWTP}	the change in flow rate at the wastewater treatment plant	m^3
P_{WWTP}	the cost of stormwater treatment	EUR/m^3
a_{WWTP}	the wastewater treatment plant stormwater flow variation coefficient	-
B_{Rec}	the benefits of reusing stormwater	EUR
Q_{Rec}	the volume of stormwater reused	m^3
P_W	the price of reusing stormwater	EUR/m^3
a_{Rec}	the stormwater reuse coefficient	-

http://www.aloki.hu ● ISSN 1589 1623 (Print) ● ISSN1785 0037 (Online)
DOI: http://dx.doi.org/10.15666/aeer/2304_83178334

Experimentation results and discussion

Pollutants outflow concentrations

Insights into the impact of bioretention cell design parameters, including vegetation type, filter media characteristics and depth, inflow hydraulic, and pollutant load, can empower designers to optimize a system's performance and longevity (Wang et al., 2019; Zhao et al., 2022). This understanding can be leveraged to maximize inflow volume reduction, enhance pollutant purification efficiency for common stormwater runoff contaminants, and slow the rate of clogging (Zhou et al., 2023). Trends in pollutant concentrations in the effluent were analyzed across 40 simulated tests divided into three stages (*Figure 3*), and the effect of filler on total pollutant concentration was determined (Lian et al., 2025).

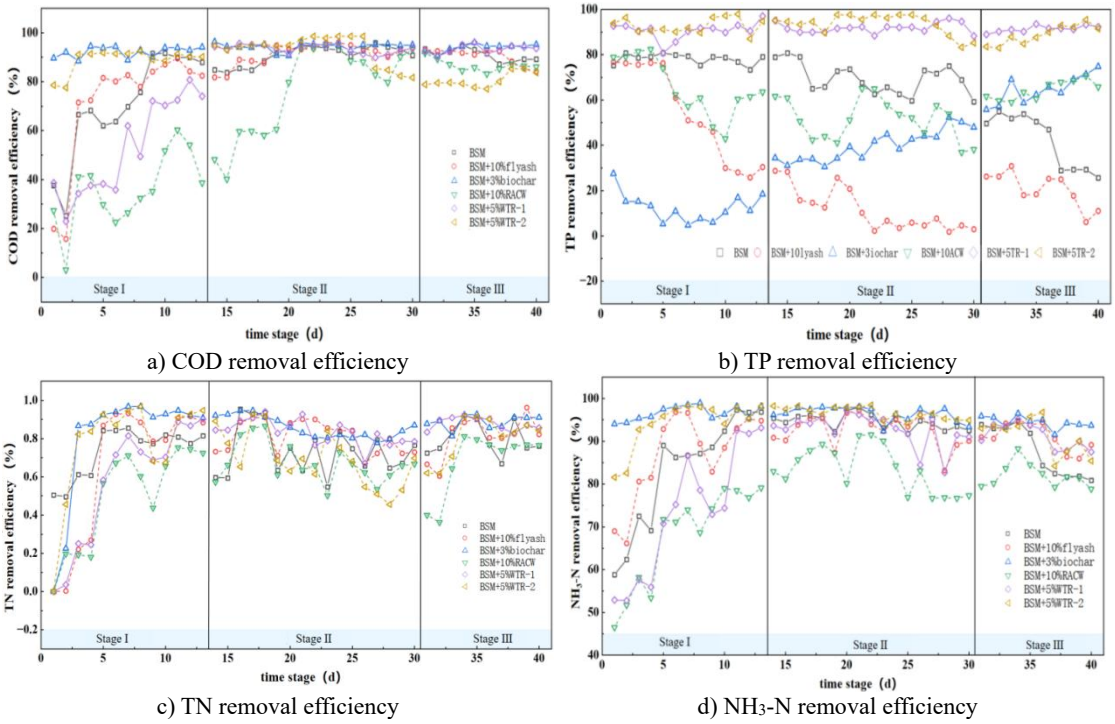

a) COD removal efficiency b) TP removal efficiency

c) TN removal efficiency d) NH_3-N removal efficiency

Figure 3. *Pollutant removal efficiency over time*

The experimental results demonstrated stable effluent pollutant concentrations during Phase II with ceased leaching, indicating optimal media purification performance (*Table 7*). The removal effect for each pollutant within all facilities exhibited considerable fluctuation, largely attributed to the combined influence of pollutants leaching and adsorption. In the second stage, the effluent concentration stabilized, with concentrations of COD, TN and TP at 16.90~60.83 (mean=27.83) mg/L, 1.07~2.38 (mean=1.71) mg/L, 0.10~1.48 (mean=0.67) mg/L, respectively. The pollutant concentration removal rates were 79.8%~98.1% (mean=94.6%), 66.0%~95.1% (mean=81.9%), 32.6%~97.7% (mean=66.2%). The WTR filler contained a large amount of Al^{3+} and Fe^{3+} and the surface voids increased after pyrolysis at a high temperature, increasing adsorption points and thus, phosphorus removal. The BET specific surface areas of WTR1 and WTR2 are 25.97 m^2/g and 256.10 m^2/g, respectively, and the cation exchange capacities (CEC) are 42.80 and 24.90 cmol/kg, both higher than other modifiers.

http://www.aloki.hu ● ISSN 1589 1623 (Print) ● ISSN1785 0037 (Online)
DOI: http://dx.doi.org/10.15666/aeer/2304_83178334

Table 7. *Change of effluent pollutant concentration (mg/L)*

		BSM	BSM+10% flyash	BSM+3% biochar	BSM+10% RACW	BSM+5% WTR-1	BSM+5% WTR-2
COD	C_{in}			300			
	C_{out}-I	72.56	72.54	22.99	186.55	124.81	31.80
	C_{out}-II	25.00	23.58	16.90	60.83	19.95	20.71
	C_{out}-III	27.35	28.78	16.50	41.78	18.75	57.96
TP	C_{in}			1.64			
	C_{out}-I	0.36	0.82	1.46	0.61	0.16	0.12
	C_{out}-II	0.51	1.48	0.97	0.80	0.13	0.10
	C_{out}-III	0.94	1.29	0.58	0.58	0.14	0.18
TN	C_{in}			7.0			
	C_{out}-I	1.69	2.00	1.18	3.05	2.65	1.55
	C_{out}-II	1.90	1.37	1.07	2.38	1.24	2.32
	C_{out}-III	1.36	1.26	0.82	2.11	0.86	1.30

Note: WTR-1&WTR-2 are water treatment residuals which are natural air-dried granulation and air-dried; and RACW is recycled aggregate of construction waste

In the third stage, the effluent concentration shows a slow upward trend due to the continuous increase of inflow and pollutant accumulation. The effluent COD, TN and TP concentration are 16.50~57.96 (mean=31.80) mg/L, 0.82~2.11 (mean=1.30) mg/L, and 0.14~1.29 (mean=0.62) mg/L, respectively. The removal rate of the pollutant concentration is 77.7%~94.2% (mean=88.0%), 63.2%~88.1% (mean=77.5%), and 21.3%~91.5% (mean=60.40%). The improved media show high removal rates for heavy metals Cu, Zn, Cd, and SS, with an average concentration reduction rate exceeding 90% for heavy metals and 96% for SS.

Attenuation process of media layer infiltration rates

The top layer of the filler serves as the zero point and is subsequently divided into an upper layer of 20 cm and a lower layer of 30 cm. The overall infiltration process at each stage is measured using the Mariotte flask's constant head method (Zhang, 2025). The infiltration rate of the different layers in the longitudinal direction is measured by the head of the piezometer. The stable infiltration rate across different systems and stages is obtained by fitting the data to the *Horton* infiltration equation using MATLAB. This process provides hydraulic conductivity curves for the different operational stages and filler layers (Li et al., 2009).

A comparative analysis of the infiltration processes at each stage revealed an overall attenuation trend in the infiltration rates of the improved bioretention system, with the fastest decay rate in Stage II. Results show that the infiltration coefficient of the upper layer (0~20 cm) of each system fluctuates between 1.44~1.97 mm/s, and the lower layer (20~50 cm) fluctuates between 1.38~2.06 mm/s. The infiltration coefficient of the upper layer in each system is lower than the lower layer. The pollutants in the inflow are primarily absorbed and accumulated in the upper layer, reducing the porosity of the upper layer media. The lower layer, with fewer accumulated pollutants, exhibits a higher infiltration rate. An exponential relationship was observed between the service time (plotted on the x-axis) and the overall stable infiltration rate (plotted on the y-axis), indicating a strong correlation (R^2>0.905) (Table 8). In systems with different improved filler media, variations in factors such as particle size, porosity, and organic matter

http://www.aloki.hu ● ISSN 1589 1623 (Print) ● ISSN1785 0037 (Online)
DOI: http://dx.doi.org/10.15666/aeer/2304_83178334

content lead to differences in performance (*Table 2*). Specifically, systems with RACW and air-dried WTR as modifiers exhibit higher stable infiltration rates and attenuation rates compared to other modified filler media.

Particle gradation of filler layers

The removal of pollutants during continuous rainfall is primarily driven by adsorption and interception mechanisms. As the system operates, the particle grading of each layer of the media may undergo changes, potentially influencing the infiltration process and generating a layering effect. To understand these dynamics, the system filler was sampled every 10 cm from the top down, providing detailed insights into the system's behavior across different layers (*Figure 4*).

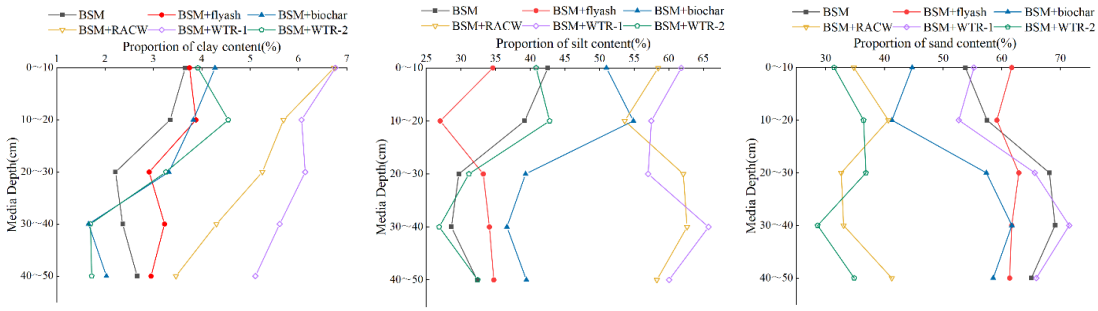

(a) Clay content (b) Silt content (c) Sand content

Figure 4. *Particle grading of different layers. Note: BSM is basic filler (mixture of river sand, planting soil and compost); WTR-1&WTR-2 are water treatment residuals which are natural air-dried granulation and air-dried; and RACW is recycled aggregate of construction waste*

Prior to the operation of the system, the distribution of clay, silt, and sand within individual sets of improved media was evenly distributed at different heights in the longitudinal direction. After 20 years of precipitation in Xi'an, the particle grading of the media in each system underwent reconfiguration under the combined influence of inflow hydraulic load, pollution load, and filler characteristics (such as porosity, particle grading, and adsorption capacity). There is a significant variation in the distribution of clay, silt, and sand content, with the overall clay content being less than 7%, showing a downward trend from top to bottom. The filler is divided into an upper layer (20 cm) and lower layer (30 cm). Experimental results indicate that the upper layer has a greater clay and silt content than the lower layer, whereas the sand content in the upper layer is significantly lower than in the lower layer (*Figure 4*).

Longitudinal accumulation and distribution of runoff pollutants

The concentrations of carbon, nitrogen, phosphorus, and heavy metals present in the system filler can reflect the extent and location of media clogging. Following the experiment, the cumulative pollutant load for different media layers was assessed (*Figure 5*).

The cumulative amount of each pollutant shows that the upper layer exceeds the lower layer. Specifically, the upper filler (0~20 cm) contains TN at 0.86~2.51 g/kg, TP at 1.12~3.99 g/kg, and TOC at 9.31~17.88 g/kg. The contents of TN, TP and TOC in the lower layer of filler (20~50 cm) are 0.75~2.33 g/kg, 0.95~2.61 g/kg and 7.13~16.03 g/kg,

http://www.aloki.hu ● ISSN 1589 1623 (Print) ● ISSN1785 0037 (Online)
DOI: http://dx.doi.org/10.15666/aeer/2304_83178334

respectively (*Figure 5a*). Among these, the TN content across different layers and systems shows a minor variation. The adsorption and interception have a less pronounced effect on TN removal than on TP and organic pollutants. Biotransformation is likely to play a crucial role in TN reduction. In terms of heavy metals, the upper filler (0~20 cm) contains Cu, Zn and Cd at 36.85~65.42 mg/kg, 115.67~242.57 mg/kg, and 4.48~16.49 mg/kg; and in the lower filler (20~50 cm) at 24.24~32.34 mg/kg, 68.02~89.06 mg/kg, and 0.44~1.37 mg/kg, respectively (*Figure 5b*). The accumulation of pollutants in the upper filler layer is greater than in the lower layer, and the accumulation of heavy metals in the upper filler is particularly notable. The accumulation of TN, TP, and TOC in the lower filler decreased by 9.3%, 21.0%, and 14.8%, respectively. The accumulation of Cu, Zn, and Cd in the lower filler decreased by 41.7%, 47.2%, and 90.0%, respectively.

		0~10cm	10~20cm	20~30cm	30~40cm	40~50cm
BSM	TP	1.25	0.98	1.03	0.91	0.9
	TN	2.54	2.48	2.26	2.43	2.31
	TOC	13.29	12.9	11.04	10.71	9.66
BSM+10% flyash	TP	1.91	2.25	1.73	1.76	1.85
	TN	0.95	0.77	0.71	0.82	0.73
	TOC	8.76	9.86	5.67	7.63	8.09
BSM+3% biochar	TP	2.93	3.08	2.43	2.29	2.24
	TN	1.28	0.97	1.06	1.12	1.07
	TOC	16.04	19.72	14.86	17.8	15.43
BSM+10% RACW	TP	4.31	3.67	2.48	2.4	2.95
	TN	1.37	1.16	1.14	1.12	0.94
	TOC	9.97	11.06	9.07	9.47	8.92
BSM+5% WTR-1	TP	2.62	2.95	2.23	2.32	2.36
	TN	1.5	1.38	1.35	1.16	1.25
	TOC	12.45	10.56	10.41	10.14	9.75
BSM+5% WTR-2	TP	2.66	2.27	2.26	2.19	2.2
	TN	1.22	1.21	1.11	1.2	1.03
	TOC	10.77	9.67	9.65	8.51	8.65

(a) Accumulation of conventional pollutants at different heights of the media (g/kg)

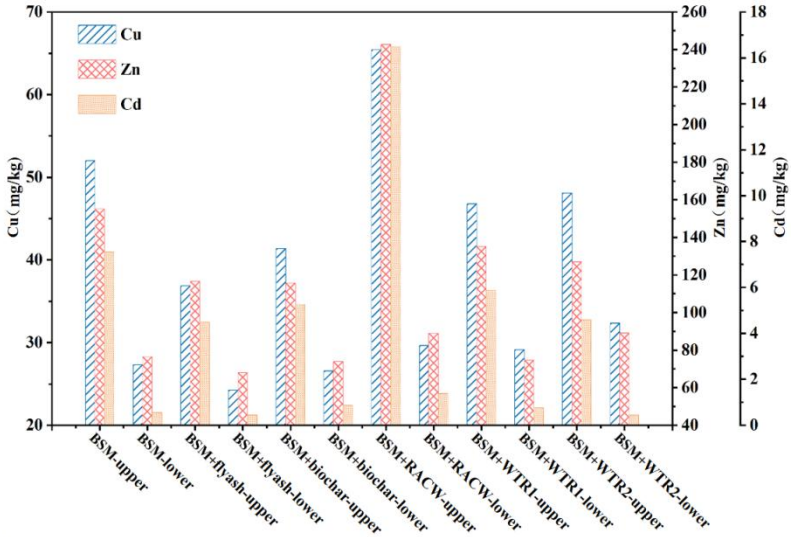

(b) Accumulation of heavy metal pollutants at different heights of the media (g/kg)

Figure 5. *Accumulation of runoff pollutants at different heights of filler media (g/kg). Note: BSM is basic filler (mixture of river sand, planting soil and compost); WTR-1&WTR-2 are water treatment residuals which natural air-dried granulation and air-dried; and RACW is recycled aggregate of construction waste*

http://www.aloki.hu ● ISSN 1589 1623 (Print) ● ISSN1785 0037 (Online)
DOI: http://dx.doi.org/10.15666/aeer/2304_83178334

Life cycle environmental impact and benefits

Life cycle environmental impact assessment

During the operation of bioretention cell systems, the steady infiltration rate of filter media continuously declines due to pollutant deposition. The system is considered to reach its end-of-life when the steady infiltration rate decreases to a threshold value. According to *Technical Specification for Stormwater Bioretention Facility (T/CUWA 40052-2022)*, the stable infiltration rate of bioretention soil media should range from 12.5 mm/h to 150.0 mm/h. In bioretention systems, a steady infiltration rate below 12.5 mm/h is considered indicative of system clogging, marking the end of the facility's service life. Based on the experimental results (*Table 8*), the service life of each bioretention cell is calculated as follows: BSM (17.0 years), BSM+10%fly ash (24.5 years), BSM+3%biochar (16.2 years), BSM+10%RACW (26.8 years), BSM+5%WTR-1 (19.2 years), and BSM+5%WTR-2 (20.4 years).

Table 8. *Stable infiltration rate of different systems at different stages (mm/h)*

	Initial stage	First stage	Second stage	Third stage	Attenuation function
BSM	60.60	56.58	11.61	9.98	$y=73.229e^{-0.104x}$ (R^2=0.911)
BSM+10% flyash	155.60	83.01	13.38	12.34	$y=160.42e^{-0.14x}$ (R^2=0.952)
BSM+3% biochar	32.30	31.50	15.55	8.128	$y=38.751e^{-0.07x}$ (R^2=0.905)
BSM+10% RACW	440.50	256.60	61.84	30.93	$y=492.65e^{-0.137x}$ (R^2=0.991)
BSM+5% WTR1	289.10	65.37	18.69	14.48	$y=219.11e^{-0.149x}$ (R^2=0.947)
BSM+5% WTR2	119.60	83.06	27.80	11.12	$y=141.11e^{-0.119x}$ (R^2=0.968)

Note: x is the service life; y is the stable infiltration rate; the attenuation function is independent of the stable infiltration rate at the initial stage and the end of the three stages; WTR-1&WTR-2 are water treatment residuals which are natural air-dried granulation and air-dried; and RACW is recycled aggregate of construction waste

The environmental impact assessment of bioretention systems is conducted on a per-unit-volume basis. The raw material acquisition and construction phases include the environmental impacts from the production of raw materials for each bioretention system (excluding amendment acquisition). It is assumed that the transportation distance for all materials is 30 kilometers, with diesel-powered freight trains used for transportation. On-site operations are defined as the environmental impact of excavating 1 cubic meter of soil using diesel excavators, while the environmental impacts of filler mixing, filling, and grading are considered negligible due to manual operations; The use of recycled solid waste as a soil amendment in bioretention cell systems is regarded as a strategy to optimize positive environmental impacts; During the operation phase, the positive environmental impact is derived from the purification of runoff pollutants. Rainfall data are based on the annual average rainfall of 611.5 mm in Xi'an, and pollutant removal rates are calculated based on the stable effluent data from Stage II in *Table 6*. The service life is determined as previously calculated; For the demolition and disposal phase, it is assumed that 80% of the scrapped materials are recycled, and the resources and energy consumed during this stage are calculated based on 90% of the construction stage (Liang, 2012). Based on these parameters, the total pollutant removal volume throughout the life cycle of the bioretention cell is calculated.

http://www.aloki.hu ● ISSN 1589 1623 (Print) ● ISSN1785 0037 (Online)
DOI: http://dx.doi.org/10.15666/aeer/2304_83178334

Open LCA is an open-source Life Cycle Assessment (LCA) software, widely used for analyzing the environmental impacts of products or services throughout their entire life cycle, from cradle to grave (Dhivya et al., 2022). The calculated data is inputted into OpenLCA, which computes the environmental impact factor values for different amendment-filled bioretention systems throughout their life cycles using a self-built database (ecoinvent 3.9 version). The negative environmental impacts occur during the raw material acquisition and construction phases, as well as the demolition and disposal phase (*Figure 6a*); The positive environmental impacts emerge during the amendment acquisition phase (*Figure 6b*); and the operation phase (*Figure 6c*).

Impact Factor	BSM	BSM+10%flyash	BSM+3%biochar	BSM+10%RACW	BSM+5%WTR-1	BSM+5%WTR-2
acidification	-2.3E+00	-2.1E+00	-2.2E+00	-2.0E+00	-2.1E+00	-2.1E+00
carcinogenic emissions	-1.7E-05	-1.6E-05	-1.6E-05	-1.5E-05	-1.6E-05	-1.6E-05
eutrophication	-1.9E+02	-1.7E+02	-1.8E+02	-1.6E+02	-1.7E+02	-1.7E+02
fossil fuel consumption	-9.7E-02	-8.4E-02	-9.1E-02	-8.4E-02	-8.9E-02	-8.9E-02
greenhouse effect	-3.6E+02	-3.3E+02	-3.5E+02	-3.3E+02	-3.4E+02	-3.4E+02
non-carcinogenic emissions	-2.6E-05	-2.3E-05	-2.6E-05	-2.2E-05	-2.4E-05	-2.4E-05
ozone depletion	-9.7E-02	-8.6E-02	-9.2E-02	-8.4E-02	-9.0E-02	-9.0E-02
respiratory impacts	-2.1E+01	-1.9E+01	-2.0E+01	-1.8E+01	-2.0E+01	-2.0E+01

(a) Environmental negative impacts

Impact Factor	BSM	BSM+10%flyash	BSM+3%biochar	BSM+10%RACW	BSM+5%WTR-1	BSM+5%WTR-2
acidification	0.0E+00	2.7E-01	6.0E-02	1.2E-01	7.0E-02	7.0E-02
carcinogenic emissions	0.0E+00	1.4E-06	4.6E-07	8.9E-07	5.4E-07	5.4E-07
eutrophication	0.0E+00	2.0E+01	5.0E+00	9.7E+00	5.8E+00	5.8E+00
fossil fuel consumption	0.0E+00	1.7E-02	2.6E-03	5.0E-03	3.0E-03	3.0E-03
greenhouse effect	0.0E+00	2.0E+01	9.6E+00	1.9E+01	1.1E+01	1.1E+01
non-carcinogenic emissions	0.0E+00	1.8E-06	6.8E-07	1.3E-06	8.0E-07	8.0E-07
ozone depletion	0.0E+00	5.3E-03	2.6E-03	5.0E-03	3.0E-03	3.0E-03
respiratory impacts	0.0E+00	1.7E+00	5.6E-01	1.1E+00	6.6E-01	6.6E-01

(b) Environmental positive impacts in modified media recycling and reuse phase

Impact Factor	BSM	BSM+10%flyash	BSM+3%biochar	BSM+10%RACW	BSM+5%WTR-1	BSM+5%WTR-2
acidification	1.9E-02	2.7E-02	9.0E-03	6.3E-02	2.7E-02	1.8E-02
carcinogenic emissions	9.9E-08	2.4E-07	1.3E-07	2.1E-07	5.8E-08	4.7E-08
eutrophication	2.8E+00	7.4E+00	4.1E+00	5.3E+00	1.2E+00	1.1E+00
fossil fuel consumption	6.3E-03	1.1E-02	4.5E-03	1.9E-02	7.4E-03	5.2E-03
greenhouse effect	7.1E+00	1.0E+01	3.4E+00	2.4E+01	1.0E+01	6.8E+00
non-carcinogenic emissions	8.2E-08	1.2E-07	3.9E-08	2.7E-07	1.1E-07	7.7E-08
ozone depletion	6.8E-04	9.8E-04	3.3E-04	2.3E-03	9.6E-04	6.4E-04
respiratory impacts	2.6E-01	3.7E-01	1.2E-01	8.5E-01	3.6E-01	2.4E-01

(c) Environmental positive impacts in operation phase

Figure 6. *Environmental negative and positive impacts of various bioretention systems. Note: Environmental negative impacts include those generated during the raw material acquisition and construction phase, as well as the demolition and disposal phase. Calculated based on BSM as the benchmark. The units for acidification, carcinogenic emissions, eutrophication, fossil fuel consumption, greenhouse effect, non-carcinogenic emissions, ozone depletion, and respiratory impacts are kgSO_2eq, CTUh, kgNeq, MJsurplus, kgCO_2eq, CTUh, kgCFC-11eq, kgPM2.5eq*

The results indicate that: In the calculation of environmental negative impacts during the raw material acquisition and construction phases, the types of transportation vehicles, transportation distances, and the scale and methods of on-site operations are similar across systems. Therefore, the environmental negative impacts generated are not significantly different. The differences in environmental negative impacts mainly stem from the energy consumption associated with each system's varying proportions (excluding the modified media) of bioretention cells system base material acquisition. As

http://www.aloki.hu ● ISSN 1589 1623 (Print) ● ISSN1785 0037 (Online)
DOI: http://dx.doi.org/10.15666/aeer/2304_83178334

a result, the environmental negative impacts in this phase are numerically similar, accounting for 77% to 79% of the total environmental negative impacts.

The environmental positive impacts generated during the modified media recycling and reuse phase account for 61% to 80% of the total environmental positive impacts. The differences in environmental positive impacts in this phase are primarily due to variations in the types and quantities of recycled solid waste. Among them, the BSM+10% fly ash system generates the highest environmental positive impacts. The main reason is that fly ash is a solid fine particulate matter collected from flue gas during the coal combustion process in industries such as power generation, heat production, and supply. Coal consumption is known to cause significant environmental pollution. Therefore, the environmental impact of fly ash production is relatively severe compared to other systems. However, recycling fly ash as an amendment for bioretention systems can eliminate the environmental impacts associated with its disposal, thereby reducing environmental pollution.

The environmental positive impacts generated during the operation phase mainly depend on the environmental positive impacts derived from the attenuation and purification of stormwater runoff by each bioretention system. These impacts account for 20% to 39% of the total environmental positive impacts, with the BSM+10% RACW system showing the most significant environmental positive impacts. The systems are most effective in reducing greenhouse gas potential, ecotoxicity, and smog emissions.

During the demolition and disposal phase, since 80% of the scrapped materials are reused, the environmental negative impacts generated by each system are relatively similar, accounting for 21% to 23% of the total environmental negative impacts.

Life cycle environmental benefits calculation

Proceeding with the monetization calculation of the environmental benefits generated by the bioretention cell systems, taking a volume of 1 cubic meter as an example, the calculations are as follows:

①The ecological benefits can be calculated using *Equation 2*. According to the team's preliminary research and the local actual conditions, the following values are selected: θ is set at 0.9; the total annual rainfall is 611.5 mm; the annual average runoff reduction rate is 80% (according to *the Assessment Standard for Sponge City Construction Effect, GB/T 51345-2018*); the catchment area is 15 m² (with a confluence ratio of catchment area to facility area being 15); the value of α_{In} is 0.225; and the municipal water price (P_w) in the research area is 0.7 EUR·m⁻³. ②The environmental benefits can be calculated through Equation 3. In this calculation, P_p is taken as 0.08 EUR, N_{SS}, N_{COD}, and N_{NH_3-N} are 4, 1, and 0.8, respectively. ③Economic benefits can be calculated using Equations 4, 5 and 6. In this calculation, the value of α_{Dec} is chosen as 0.319, the value of α_{WWTP} is selected as 0.19, and the value of α_{Rec} is chosen as 0.15 (Jia, 2023). P_{Dec}, P_{WWTP}, and P_{Rec} represent prices of 0.19, 0.13, and 0.70 EUR per cubic meter (m³), respectively, all of which are local prices in the research area.

Therefore, the monetized benefits generated by BSM, BSM+10% flyash, BSM+3% biochar, BSM+10% RACW, BSM+5% WTR-1, and BSM+5% WTR-2 over their entire life cycles are 52.03 EUR·m⁻³, 73.81 EUR·m⁻³, 49.61 EUR·m⁻³, 77.44 EUR·m⁻³, 58.08 EUR·m⁻³, and 61.71 EUR·m⁻³, respectively. By using a monetization approach for quantitative calculation, the study assessed the impacts of the bioretention cells system on groundwater stability, urban water environment improvement, rainwater pollution reduction and water quality enhancement, as well as the alleviation of pressure on

http://www.aloki.hu ● ISSN 1589 1623 (Print) ● ISSN1785 0037 (Online)
DOI: http://dx.doi.org/10.15666/aeer/2304_83178334

drainage networks and wastewater treatment plant operations, and rainwater resource reuse throughout its entire life cycle. This study clarified the benefits of bioretention cells and provided theoretical support for the quantitative assessment of the benefits of bioretention cells construction.

Conclusions

Appropriate media composition and grading are key elements in bioretention design, as it directly influences operational efficiency and clogging prevention. Maintaining an optimal hydraulic conductivity indirectly increases pollutant removal by restricting runoff overflow. Temporal process of effluent concentration for solid waste modified media was revealed. Under the interaction of adsorption-desorption, the effluent concentration in stage II demonstrated relative stability and had the most efficient media purification. The attenuation process of infiltration capacity is exponential, and the contents of pollutants was higher in the upper layer. Furthermore, the clay and silt content were greater in the upper layer compared to the lower layer, whereas the sand content showed an opposite distribution. It also further clarifies the vertical layering differences in bioretention media, which holds significant value for establishing a life cycle assessment model. In the process of assessing bioretention basins, the life cycle environmental impacts of solid waste amended fillers were assessed using OpenLCA. The raw material acquisition and construction phase, and the modified media recycling and reuse phase, significantly impacts the life cycle of bioretention cells. The lifespans of the bioretention cell systems are 20.7±4.2 years, and the monetized benefits of the bioretention cell systems are 61.71±10.406 EUR·m^{-3}.

Statements and declarations. The authors declare that they have no known competing financial interests or personal relationships that could have appeared to influence the work reported in this paper.

Funding declaration. This research was financially supported by Shaanxi Water Conservancy Science and Technology Plan Project (2024SLKJ-15); and the Natural Science Basic Research Program of Shaanxi Province (2025JC-YBQN-677).

REFERENCES

[1] Brudler, S., Arnbjerg-Nielsen, K., Hauschild, M. Z. (2016): Life cycle assessment of stormwater management in the context of climate change adaptation. – Water Research 106: 394-404.
[2] Chen, Y., Chen, R. Y., Liu, Z., Ren, B. X., Wu, Q., Zhang, J., Tang, Y. H., Wu, Q. Y. (2022): Bioretention system mediated by different dry-wet alterations on nitrogen removal: Performance, fate, and microbial community. – Science of The Total Environment 827: 154295.
[3] China Urban Water Association (CUWA). (2022): Technical specification for stormwater bioretention facility. – T/CUWA 40052-2022, China.
[4] Coelho, L. M. G. (2024): Assessing the effect of local characteristics on environmental impacts of Constructed Wetlands by regionalized life cycle assessment. – Ecological Engineering 209: 107423.
[5] Dhivya, B. R., Vidjeapriya, R. (2022): Life Cycle Cost Analysis of rooftop gardens using openLCA. – IOP Conference Series: Earth and Environmental Science 1086(1).
[6] Ding, B., Rezanezhad, F., Gharedaghloo, B., Cappellen, P. V., Passeport, E. (2019): Bioretention cells under cold climate conditions: Effects of freezing and thawing on water

http://www.aloki.hu ● ISSN 1589 1623 (Print) ● ISSN1785 0037 (Online)
DOI: http://dx.doi.org/10.15666/aeer/2304_83178334

infiltration, soil structure, and nutrient removal. – Science of The Total Environment 649: 749-759.
[7] Flynn, K. M., Traver, R. G. (2013): Green infrastructure life cycle assessment: A bio-infiltration case study. – Ecological Engineering 55: 9-22.
[8] Guo, C., Li, J. K., Ma, Y., Li, H. E., Yuan, M., Ji, G. Q. (2018): Fate analysis and value estimation for rain gardens. – Acta Scientiae Circumstantiae 38(11): 3-9. (in Chinese).
[9] Haghani, I., Shokohi, T., Hajheidari, Z., Khalilian, A., Aghili, S. R. (2013): Comparison of Diagnostic Methods in the Evaluation of Onychomycosis. – Mycopathologia 175(3-4): 315-321.
[10] Hatt, B. E., Fletcher, T. D., Deletic, A. (2007): Hydraulic and pollutant removal performance of stormwater filters under variable wetting and drying regimes. – Water Science and Technology 56(12): 11-19.
[11] Iqbal, H., Garcia-Perez, M., Flury, M. (2015): Effect of biochar on leaching of organic carbon, nitrogen, and phosphorus from compost in bioretention systems. – Science of The Total Environment 521-522: 37-45.
[12] Jia, B. K. (2023): Research on comprehensive benefits of sponge city construction and its monetization method: cases of Xixian new area, Shaanxi and Guyuan, Ningxia. – Xi'an University of Technology, pp. 59-84. (in Chinese).
[13] Kheiralipour, K., Rafiee, S., Karimi, M., Nadimi, M., Paliwal, J. (2023): The environmental impacts of commercial poultry production systems using life cycle assessment: a review. – World's Poultry Science Journal 80(1): 33-54.
[14] Li, H., Davis, A. P. (2008a): Urban Particle Capture in bioretention media. I: Laboratory and field studies. – Journal of Environmental Engineering 134(6): 409-418.
[15] Li, H., Davis, A. P. (2008b): Urban Particle Capture in bioretention media. II: Theory and Model Development. – Journal of Environmental Engineering 134(6): 419-432.
[16] Li, Z., Wu, P., Feng, H., Zhao, X. N., Huang, J., Zhuang, W. H. (2009): Simulated experiment on effect of soil bulk density on soil infiltration capacity. – Transactions of the CSAE 25(6): 40-45. (in Chinese).
[17] Li, J., Jiang, Y. C., Li, X. (2021): Response relationship between stormwater runoff pollution reduction and source volume control. – China Water & Wastewater 37(15): 102-109. (in Chinese).
[18] Lian, X. K., Tang, Y. H., Wu, Q., Xiao, H. J., Ni, J. H., Yuan, Y., Wang, Q. Y., Zhen, L., Zou, G. J., Zhang, S. X., Meng, C. H., Chen, Y. (2025): Application of construction waste residue-based compositing fillers in bioretention facility: Intensified nitrogen removal and mitigated by-product effects. – Environmental Research 274: 121315.
[19] Liang, S. (2012): Research on the environmental impact load of the urban wastewater treatment plant by the method of life cycle assessment. – Harbin Institute of Technology 21-38. (in Chinese).
[20] Lisenbee, W. A., Hathaway, J. M., Burns, M. J., Fletcher, T. D. (2021): Modeling bioretention stormwater systems: Current models and future research needs. – Environmental Modelling & Software 144: 105146.
[21] Ministry of Housing and Urban-Rural Development of the People's Republic of China & State Administration for Market Regulation of the People's Republic of China. (2018): Assessment standard for sponge city construction effect. – GB/T 51345-2018, China.
[22] Moon, S. K., Woo, N. C., Lee, K. S. (2004): Statistical analysis of hydrographs and water-table fluctuation to estimate groundwater recharge. – Journal of Hydrology 292(1-4): 198-209.
[23] Moore, T. L. C., Hunt, W. F. (2013): Predicting the carbon footprint of urban stormwater infrastructure. – Ecological Engineering 58: 44-51.
[24] Nabiul Afrooz, A. R. M., Boehm, A. B. (2017): Effects of submerged zone, media aging, and antecedent dry period on the performance of biochar-amended biofilters in removing fecal indicators and nutrients from natural stormwater. – Ecological Engineering 102: 320-330.

http://www.aloki.hu ● ISSN 1589 1623 (Print) ● ISSN1785 0037 (Online)
DOI: http://dx.doi.org/10.15666/aeer/2304_83178334

[25] National People's Congress of the People's Republic of China. (2016): Environmental Protection Tax Law of the People's Republic of China. – Effective from January 1, 2018.
[26] Pourmehdi, K., Kheiralipour, K. (2023): Compression of input to total output index and environmental impacts of dryland and irrigated wheat production systems. – Ecological Indicators 148: 110048.
[27] Ryberg, M., Vieira, M. D. M., Zgola, M., Bare, J., Rosenbaum, R. K. (2014): Updated US and Canadian normalization factors for TRACI 2.1. – Clean Techn Environ Policy 16: 329-339.
[28] Tirpak, R. A., Nabiul Afrooz, A. R. M., Winston, R. J., Valenca, R., Schiff, K., Mohanty, S. K. (2021): Conventional and amended bioretention soil media for targeted pollutant treatment: A critical review to guide the state of the practice. – Water Research 189: 116648.
[29] Vijayaraghavan, K., Biswal, B. K., Adam, M. G., Soh, S. H., Tsen-Tieng, D. L., Davis, A. P., Chew, S. H., Tan, P. Y., Babovic, V., Balasubramanian, R. (2021): Bioretention systems for stormwater management: Recent advances and future prospects. – Journal of Environmental Management 292: 112766.
[30] Wan, Z. X., Li, T., Shi, Z. B. (2017): A layered bioretention system for inhibiting nitrate and organic matters leaching. – Ecological Engineering 107: 233-238.
[31] Wang, L. (2008): Study on drainage charge system and application research. – Chang'an University (in Chinese).
[32] Wang, J., Chua, L. H. C., Shanahan, P. (2019): Hydrological modeling and field validation of a bioretention basin. – Journal of Environmental Management 240: 149-159.
[33] Wang, H. K. (2023): Study on permeability characteristics and infiltration mechanism of loess under the influence of major engineering. – Chang'an University, pp. 38-59. (in Chinese).
[34] Wardynski, B. J., Hunt, W. F. (2012): Are bioretention cells being installed per design standards in North Carolina? A field study. – Journal of Environmental Engineering 138(12): 1210-1217.
[35] Xu, C. Q., Lin, W., Zhu, Y. F., Zhang, B., Wang, Z. H., Jia, H. F. (2024): A macro-level life-cycle environmental-economic impact and benefit assessment of sponge cities in China. – Resources, Conservation and Recycling 211: 107859.
[36] Zhang, L., Jiang, X., Sun, R., Cui, C. Y., Gu, H. Y., Qiu, Y. J. (2025): A novel analytical approach for 3D stability of unsaturated soil slopes with cracks under rainfall infiltration. – Engineering Failure Analysis 175: 109545.
[37] Zhao, H. T., Ma, Y. K., Fang, J. X., Hu, L., Li, X. Y. (2022): Particle size distribution and total suspended solid concentrations in urban surface runoff. – Science of The Total Environment 815: 152533.
[38] Zhou, J. J., Xiong, J. Q., Xie, X. F., Liu, Y. Z. (2023): Clogging mechanism of bioretention cell with fine-grained soil medium. – Journal of Water Process Engineering 53: 103630.

http://www.aloki.hu ● ISSN 1589 1623 (Print) ● ISSN1785 0037 (Online)
DOI: http://dx.doi.org/10.15666/aeer/2304_83178334